Position Sensorless Operation of IPMSM with Near PWM Switching Frequency Signal Injection

Sungmin Kim*, Yong-Cheul Kwon*, Seung-Ki Sul*, Joonho Park**, and Sang-Min Kim**
*Seoul National University, 599 Gwanangno Gwanak-gu Seoul, Korea
**Samsung Techwin R&D Center, Bundang-gu, Seongnam-si, Gyeonggi-do, Korea

***Abstract*-- This paper proposes a new position sensorless control method based on the high frequency signal injection. The frequency of the signal is increased up to 2/3 of the switching frequency, and the dynamics of the sensorless control can be improved. Furthermore, the audible noise is reduced conspicuously due to the increased frequency of injected signal. In this method, the rotor position is directly calculated from three successively sampled currents and voltages without any filter. The injected signal comes from three voltage vectors rotating at the stationary reference frame. The 15Hz speed control bandwidth and 300Hz current regulation bandwidth has been demonstrated with the experimental test results.**

***Index Terms*-- Sensorless control, Signal injection, Near PWM switching frequency, IPMSM**

I. INTRODUCTION

During last decades, position sensorless operation of Interior Permanent Magnet Synchronous Motor (IPMSM) has been investigated extensively [1]-[2]. When the rotating speed of IPMSM is high enough, the rotor position information can be estimated from voltage equations of IPMSM [2]-[4]. At standstill or very low rotating speed, however, the voltage equations have severe error due to nonlinearity of Pulse-Width-Modulation (PWM) inverter. Therefore, additional signal injection methods to detect the rotor position in standstill or low rotating speed have been proposed, and some of them have been already commercialized.

The additional voltage signal injection methods are based on the characteristics of IPMSM: the spatial inductance distribution is determined by rotor position because of inductance saliency [1]. According to the rotor position, the current response due to the injected voltage signal is defined, that means that the current values have information related to the rotor position. To get the rotor position information from the current, the current response due to the injected voltage signal is analyzed with the high frequency impedance model of IPMSM. In addition to those analysis results, proper demodulation processes to extract the meaningful information from the measured currents have been incorporated. At first, the ordinary demodulation process is a heterodyning method, which extracts the injection frequency component from the measured phase current and decouples the position related information from the extracted component. In this heterodyning method, the Band-Pass-Filters (BPFs) and Low-Pass-Filters (LPFs) are required [1],[5]. The design of these filters is not easy task and also these filters limit the upper bound of the frequency of injection signal. Fig. 1 shows a typical signal processing block diagram of the voltage signal injection sensorless method using heterodyning demodulation process.

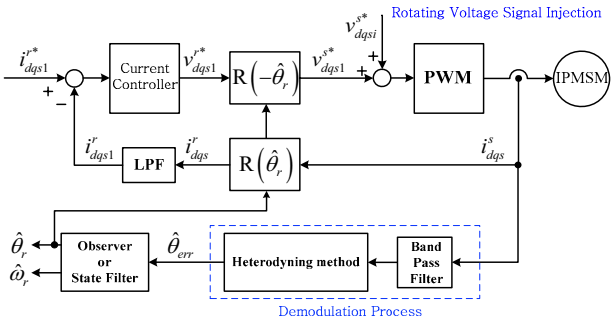

Fig. 1. Block diagram of the conventional rotating voltage signal injection method using heterodyning demodulation

The signal injection sensorless methods can be divided into two groups according to the injected voltage signal types: the rotating signal injection in the stationary reference frame [1], and the pulsating signal injection in the rotating reference frame [5]-[6], [10]-[11]. The former injects the rotating voltage signal spatially regardless of the rotor position and the latter at the estimated rotor position. These sensorless methods have unique characteristics according to the injected signal type. Those affect the rotor position detection performance, and many research results have reported the relationships between sensorless methods and sensorless performance [12]-[19].

Meanwhile, some sensorless methods have chosen a square wave voltage signal as the injection signal [7]-[11]. In these cases, the frequency of the injection voltage signal is ordinary high: from half of PWM switching frequency to PWM switching frequency. In [10]-[11], the injection frequency is a half of PWM switching frequency and the signal type is pulsating voltage signal in the estimated rotor reference frame. In [8], [9], the injection frequency is PWM switching frequency and the signal type is rotating voltage signal in the stationary reference frame. To inject the rotating voltage signal in PWM switching frequency, the PWM pattern was modified according to each demodulation method. This PWM modification needs additional complexity in current control and raises current sampling issues.

Even though all sensorless methods have unique characteristics in the injection signal type or in the demodulation technique, the rotor position in every sensorless method is obtained from the current response by the corresponding the injected voltage signal.

978-1-61284-957-7/11/$26.00 ©2011 IEEE

However, the current contain not only current ripple due to the intentionally injected voltage signal, but also extra current ripple by the fundamental current control or other unexpected phenomenon. To get the position information exactly, therefore, the only current ripple by the corresponding the injected voltage should be extracted from the measured phase current.

As a way to get the exact rotor position information, the injection frequency can be increased. If the frequency of the injected signal is getting higher, the dynamics of the sensorless control can be improved and the interference between the injected signal and the fundamental components of the current for torque control can be reduced. Furthermore, if the injected frequency is increased near or above 15kHz, the audible noise can be reduced conspicuously. This paper proposed a new demodulation method to extract the rotor position information exactly even though the injection frequency is two third of PWM switching frequency. This method is a kind of a direct calculation of spatial information from stationary inductance matrix and does not use any signal processing filter except a weak low pass filter to remove high frequency signal noise. Because the injection frequency is very far from the current control bandwidth, the precise and fast position detection is possible even in the transient state.

II. High Frequency Rotating Signal Injection Method

Conventionally, the heterodyning method has been used as the demodulation process of the rotating voltage signal injection sensorless method. In heterodyning method, the extraction of the current component at the injected frequency and Phase-Locked-Loop (PLL) multiplication in the injection frequency are necessary. To extract the injection frequency component from phase currents, Band-Pass-Filter (BPF) is often used. As the frequency of the injection signal is getting higher, the number of sampling for a period of the injected signal is getting smaller. Because of this smaller sampling number, the implementation of BPF in discrete form is difficult, and the performance of the filter is getting degraded.

By exploiting the difference of the measured current, the spatial information can be directly calculated without any high frequency filter. Eq. (1) is the voltage equation of IPMSM in the stationary d-/q-axis reference frame. The flux in stationary reference frame, (λ_{ds}^s, λ_{qs}^s) are function of currents, the flux linkage of the rotor permanent magnet, and the inductance matrix, L_S as (2). The inductance matrix, L_S, can be derived with d-/q-axis inductance, (L_{ds}, L_{qs}) in rotor reference frame and rotor position, θ_r in (3). Because of the saliency of IPMSM, the inductance matrix, L_S has the spatial information of the rotor. Therefore, the rotor position, θ_r can be extracted from inductance matrix information.

From the voltage equations of IPMSM, the inductance matrix can be derived. The voltage equations can be rewritten from (1)-(3) as (4). The voltage in (4) can be considered as sum of two components, namely, fundamental voltage (v_{dsf}^s, v_{qsf}^s), and current control voltage (v_{dsc}^s, v_{qsc}^s): the former comes from the resistance drop voltage and back-EMF voltage, and the latter from the voltage generated by the current controller to regulate the fundamental current. Therefore, the voltage reference of PWM inverter for IPMSM drives is the sum of fundamental voltage (v_{dsf}^s, v_{qsf}^s) in (5) and current control voltage (v_{dsc}^s, v_{qsc}^s) in (6).

$$\begin{bmatrix} v_{ds}^s \\ v_{qs}^s \end{bmatrix} = R_s \begin{bmatrix} i_{ds}^s \\ i_{qs}^s \end{bmatrix} + \frac{d}{dt}\begin{bmatrix} \lambda_{ds}^s \\ \lambda_{qs}^s \end{bmatrix}. \tag{1}$$

$$\begin{bmatrix} \lambda_{ds}^s \\ \lambda_{qs}^s \end{bmatrix} = L_s \begin{bmatrix} i_{ds}^s \\ i_{qs}^s \end{bmatrix} + \lambda_f \begin{bmatrix} \cos\theta_r \\ \sin\theta_r \end{bmatrix}. \tag{2}$$

$$L_s = \begin{bmatrix} \Sigma L + \Delta L\cos 2\theta_r & \Delta L\sin 2\theta_r \\ \Delta L\sin 2\theta_r & \Sigma L - \Delta L\cos 2\theta_r \end{bmatrix}$$
$$\Sigma L = \frac{L_{ds}+L_{qs}}{2} \qquad \Delta L = \frac{L_{ds}-L_{qs}}{2}. \tag{3}$$

$$\begin{bmatrix} v_{ds}^s \\ v_{qs}^s \end{bmatrix} = R_s \begin{bmatrix} i_{ds}^s \\ i_{qs}^s \end{bmatrix} + L_S \frac{d}{dt}\begin{bmatrix} i_{ds}^s \\ i_{qs}^s \end{bmatrix} + \lambda_f \begin{bmatrix} -\omega_r \sin\theta_r \\ \omega_r \cos\theta_r \end{bmatrix} + \begin{bmatrix} -2\omega_r \Delta L\sin 2\theta_r & 2\omega_r \Delta L\cos 2\theta_r \\ 2\omega_r \Delta L\cos 2\theta_r & 2\omega_r \Delta L\sin 2\theta_r \end{bmatrix}\begin{bmatrix} i_{ds}^s \\ i_{qs}^s \end{bmatrix}. \tag{4}$$

$$\begin{bmatrix} v_{dsf}^s \\ v_{qsf}^s \end{bmatrix} = R_s \begin{bmatrix} i_{dsf}^s \\ i_{qsf}^s \end{bmatrix} + \omega_r \left(L_C(\theta)\begin{bmatrix} i_{dsf}^s \\ i_{qsf}^s \end{bmatrix} + \lambda_f \begin{bmatrix} -\sin\theta_r \\ \cos\theta_r \end{bmatrix} \right). \tag{5}$$

$$\begin{bmatrix} v_{dsc}^s \\ v_{qsc}^s \end{bmatrix} = L_S \frac{1}{\Delta T}\begin{bmatrix} i_{dsc}^s \\ i_{qsc}^s \end{bmatrix}. \tag{6}$$

To extract the rotor position information from inductance matrix, L_S, the arbitrary high frequency voltage signal can be added to the fundamental voltage reference from current controller. Then, the voltage (v_{ds}^s, v_{qs}^s) to IPMSM is the sum of output voltage from current controller ($v_{dsf}^s + v_{dsc}^s$, $v_{qsf}^s + v_{qsc}^s$) and the high frequency injection voltage (v_{dsi}^s, v_{qsi}^s). And to extract the spatial information, the value of the inductance matrix, L_S, should be obtained. The current variation can be caused by two kind of voltage: current control voltage (v_{dsc}^s, v_{qsc}^s) and injection voltage (v_{dsi}^s, v_{qsi}^s). Ideally, the only current ripple due to the injection voltage (v_{dsi}^s, v_{qsi}^s) should be considered in the rotor position detection. However, the current ripples by two different voltages are not able to be separated easily. Therefore, the voltages to generate current ripple can be defined as the effective voltage (v_{dsh}^s, v_{qsh}^s). The effective voltage (v_{dsh}^s, v_{qsh}^s) is the sum of the current control voltage (v_{dsc}^s, v_{qsc}^s) in (6) and the injection voltage (v_{dsi}^s, v_{qsi}^s) in (7), which can be derived from (4). Finally, the voltage reference from PWM inverter consists of the fundamental voltage (v_{dsf}^s, v_{qsf}^s) and the current variation voltage (v_{dsh}^s, v_{qsh}^s) in (7) and (8). And the current variation is generated by the current variation voltage as (9).

$$\begin{bmatrix} v_{ds}^s \\ v_{qs}^s \end{bmatrix} = \left(\begin{bmatrix} v_{dsf}^s \\ v_{qsf}^s \end{bmatrix} + \begin{bmatrix} v_{dsc}^s \\ v_{qsc}^s \end{bmatrix} \right) + \begin{bmatrix} v_{dsi}^s \\ v_{qsi}^s \end{bmatrix}$$
$$= \begin{pmatrix} R_s \begin{bmatrix} i_{dsf}^s \\ i_{qsf}^s \end{bmatrix} + L_S \frac{1}{\Delta T} \begin{bmatrix} \Delta i_{dsc}^s \\ \Delta i_{qsc}^s \end{bmatrix} \\ +\omega_r \left(L_C(\theta) \begin{bmatrix} i_{dsf}^s \\ i_{qsf}^s \end{bmatrix} + \lambda_f \begin{bmatrix} -\sin\theta_r \\ \cos\theta_r \end{bmatrix} \right) \end{pmatrix} + L_S \frac{1}{\Delta T} \begin{bmatrix} \Delta i_{dsi}^s \\ \Delta i_{qsi}^s \end{bmatrix}. \quad (7)$$

$$\begin{bmatrix} v_{ds}^s \\ v_{qs}^s \end{bmatrix} = \begin{bmatrix} v_{dsf}^s \\ v_{qsf}^s \end{bmatrix} + \left(\begin{bmatrix} v_{dsc}^s \\ v_{qsc}^s \end{bmatrix} + \begin{bmatrix} v_{dsi}^s \\ v_{qsi}^s \end{bmatrix} \right) = \begin{bmatrix} v_{dsf}^s \\ v_{qsf}^s \end{bmatrix} + \begin{bmatrix} v_{dsh}^s \\ v_{qsh}^s \end{bmatrix}. \quad (8)$$

$$\begin{bmatrix} v_{dsh}^s \\ v_{qsh}^s \end{bmatrix} = L_S \frac{1}{\Delta T} \begin{bmatrix} \Delta i_{dsh}^s \\ \Delta i_{qsh}^s \end{bmatrix}. \quad (9)$$

The inductance matrix, L_S, where the rotor position related spatial information is contained, can be obtained from the current variation voltage and the current variation in (9). However, it is very difficult to extract the only current variation voltage, (v_{dsh}^s, v_{qsh}^s) from the voltage reference, (v_{ds}^s, v_{qs}^s). In this paper, voltage difference modulation method is proposed. Eq. (10) and (12) show the voltage equations of the two successive sampling instances. Because the sampling interval is small enough, the fundamental voltages and currents of the two successive sampling as (11) and (13) can be considered as constant value under the assumption of no variation of rotor position for a sampling interval. Then, by subtraction (11) from (10) the voltage difference equation, which is related to the only current variation voltage, can be extracted in (14). The current variation can be measured by current sampling in every sampling instance.

$$\begin{bmatrix} v_{ds1}^s \\ v_{qs1}^s \end{bmatrix} = \begin{bmatrix} v_{dsf1}^s \\ v_{qsf1}^s \end{bmatrix} + \begin{bmatrix} v_{dsh1}^s \\ v_{qsh1}^s \end{bmatrix} = \begin{bmatrix} v_{dsf1}^s \\ v_{qsf1}^s \end{bmatrix} + L_S \frac{1}{\Delta T} \begin{bmatrix} \Delta i_{dsh1}^s \\ \Delta i_{qsh1}^s \end{bmatrix}. \quad (10)$$

$$\begin{bmatrix} v_{dsf1}^s \\ v_{qsf1}^s \end{bmatrix} = R_s \begin{bmatrix} i_{dsf1}^s \\ i_{qsf1}^s \end{bmatrix} + \omega_r \left(L_C(\theta) \begin{bmatrix} i_{dsf1}^s \\ i_{qsf1}^s \end{bmatrix} + \lambda_f \begin{bmatrix} -\sin\theta_r \\ \cos\theta_r \end{bmatrix} \right). \quad (11)$$

$$\begin{bmatrix} v_{ds2}^s \\ v_{qs2}^s \end{bmatrix} = \begin{bmatrix} v_{dsf2}^s \\ v_{qsf2}^s \end{bmatrix} + \begin{bmatrix} v_{dsh2}^s \\ v_{qsh2}^s \end{bmatrix} = \begin{bmatrix} v_{dsf2}^s \\ v_{qsf2}^s \end{bmatrix} + L_S \frac{1}{\Delta T} \begin{bmatrix} \Delta i_{dsh2}^s \\ \Delta i_{qsh2}^s \end{bmatrix}. \quad (12)$$

$$\begin{bmatrix} v_{dsf2}^s \\ v_{qsf2}^s \end{bmatrix} = R_s \begin{bmatrix} i_{dsf2}^s \\ i_{qsf2}^s \end{bmatrix} + \omega_r \left(L_C(\theta) \begin{bmatrix} i_{dsf2}^s \\ i_{qsf2}^s \end{bmatrix} + \lambda_f \begin{bmatrix} -\sin\theta_r \\ \cos\theta_r \end{bmatrix} \right) \quad (13)$$

$$\begin{bmatrix} v_{ds2}^s - v_{ds1}^s \\ v_{qs2}^s - v_{qs1}^s \end{bmatrix} = \begin{bmatrix} v_{dsh2}^s - v_{dsh1}^s \\ v_{qsh2}^s - v_{qsh1}^s \end{bmatrix} = L_S \frac{1}{\Delta T} \begin{bmatrix} \Delta i_{dsh2}^s - \Delta i_{dsh1}^s \\ \Delta i_{qsh2}^s - \Delta i_{qsh1}^s \end{bmatrix} \quad (14)$$
$$\left(\because \begin{bmatrix} v_{dsf1}^s \\ v_{qsf1}^s \end{bmatrix} \approx \begin{bmatrix} v_{dsf2}^s \\ v_{qsf2}^s \end{bmatrix}, \begin{bmatrix} i_{dsf1}^s \\ i_{qsf1}^s \end{bmatrix} \approx \begin{bmatrix} i_{dsf2}^s \\ i_{qsf2}^s \end{bmatrix} \right).$$

Because the inductance matrix, L_S is 2 by 2 matrix, two sets of (14) should be needed to calculate the inductance matrix, L_S. Therefore, the voltages and currents at three successive sampling instances, namely (v_{ds1}^s, v_{qs1}^s), (v_{ds2}^s, v_{qs2}^s) and (v_{ds3}^s, v_{qs3}^s) is used to get two voltage differences and the corresponding current differences as described in (15). From (15), the inductance matrix can be deduced as (16). From (16), the rotor position information, θ_r can be derived as (18).

$$\begin{bmatrix} v_{ds32}^s & v_{ds21}^s \\ v_{qs32}^s & v_{qs21}^s \end{bmatrix} = \begin{bmatrix} v_{ds3}^s - v_{ds2}^s & v_{ds2}^s - v_{ds1}^s \\ v_{qs3}^s - v_{qs2}^s & v_{qs2}^s - v_{qs1}^s \end{bmatrix}$$
$$= L_S \frac{1}{\Delta T} \begin{bmatrix} \Delta i_{dsh3}^s - \Delta i_{dsh2}^s & \Delta i_{dsh2}^s - \Delta i_{dsh1}^s \\ \Delta i_{qsh3}^s - \Delta i_{qsh2}^s & \Delta i_{qsh2}^s - \Delta i_{qsh1}^s \end{bmatrix} \quad (15)$$
$$= L_S \frac{1}{\Delta T} \begin{bmatrix} \Delta i_{dsh32}^s & \Delta i_{dsh21}^s \\ \Delta i_{qsh32}^s & \Delta i_{qsh21}^s \end{bmatrix}.$$

$$L_S = \begin{bmatrix} \Sigma L + L_1 \cos 2\theta_r & \Delta L \sin 2\theta_r \\ \Delta L \sin 2\theta_r & \Sigma L - \Delta L \cos 2\theta_r \end{bmatrix}$$
$$= \Delta T \begin{bmatrix} v_{ds32}^s & v_{ds21}^s \\ v_{qs32}^s & v_{qs21}^s \end{bmatrix} \begin{bmatrix} \Delta i_{dsh32}^s & \Delta i_{dsh21}^s \\ \Delta i_{qsh32}^s & \Delta i_{qsh21}^s \end{bmatrix}^{-1} = \begin{bmatrix} L_{11} & L_{12} \\ L_{21} & L_{22} \end{bmatrix}. \quad (16)$$

$$\begin{aligned} L_{12} + L_{21} &= 2\Delta L \sin 2\theta_r \\ L_{11} - L_{22} &= 2\Delta L \cos 2\theta_r \end{aligned}. \quad (17)$$

$$2\hat{\theta}_{rCal} = \tan^{-1}\left(\frac{L_{12} + L_{21}}{L_{11} - L_{22}} \right). \quad (18)$$

III. Implementation of Proposed Sensorless Method

To maximize the frequency of injection signal, three voltage vectors have to be chosen in one period of injection signal for three successive sampling of voltages and currents. In Fig. 2, the three injection voltage vectors with the output voltage of current controller in the stationary reference frame are shown. Because three successive independent voltage vectors are injected in one injection period, the injection frequency can be increased to two third of PWM switching frequency.

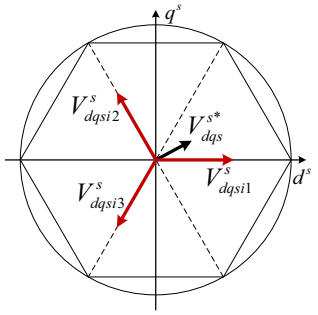

Fig. 2. Voltage reference vector and injection voltage vectors in stationary reference frame.

Fig. 3 shows the voltage reference from the current controller updated at every half of PWM switching period, the injected high frequency voltage signal whose frequency is 2/3 of the PWM switching frequency, and current sampling point. In the figure, the PWM switching frequency is 10kHz, the sampling frequency is 20kHZ, and the injection frequency is 6.67kHz. In one injection frequency period, there are three voltage vectors and three sampling points. Using these three voltage references and the corresponding phase currents, the rotor position information can be calculated as (16), (17) and (18). The overall block diagram of the proposed sensorless control is shown in Fig. 4.

Because the calculated angle from (16) and (18) is corrupted by noise, an estimator should be applied to enhance signal to noise ratio. In this paper, conventional Luenberger speed observer was adopted as shown Fig. 5(a). This observer can be replaced with a conventional state filter as shown Fig. 5(b). If an exact inertia value was known, Luenberger speed observer gives better performance in speed estimation.

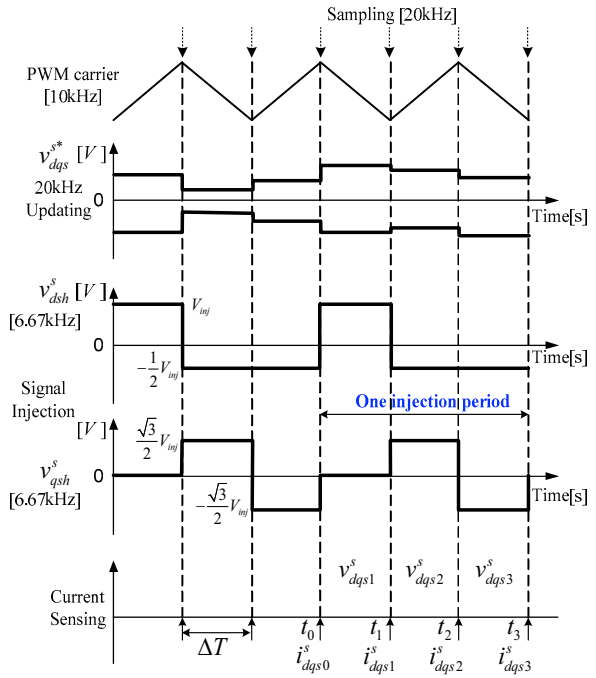

Fig. 3. PWM of voltage reference including the output voltage of current controller and injection voltage.

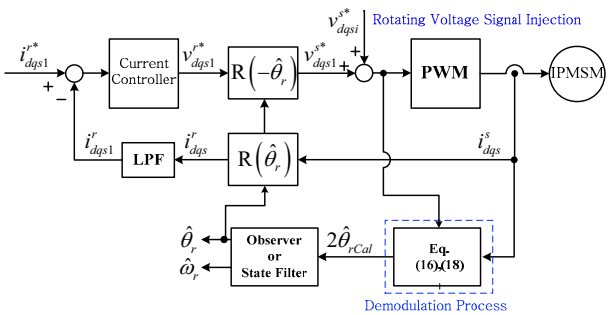

Fig. 4. Block diagram of the proposed rotating voltage signal injection method without any high frequency filters.

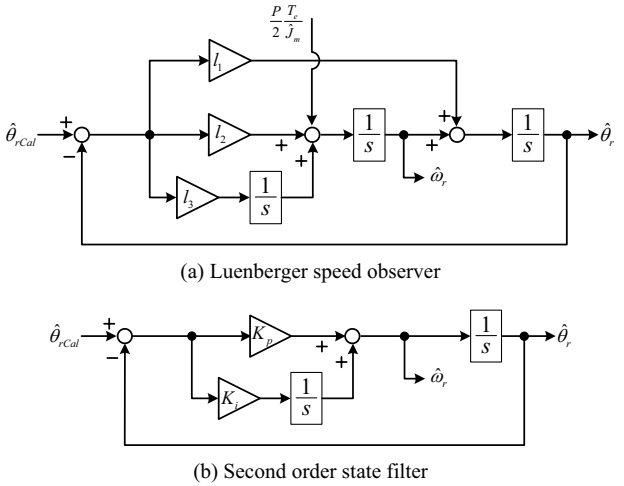

Fig. 5. Block diagram of the rotor position estimator

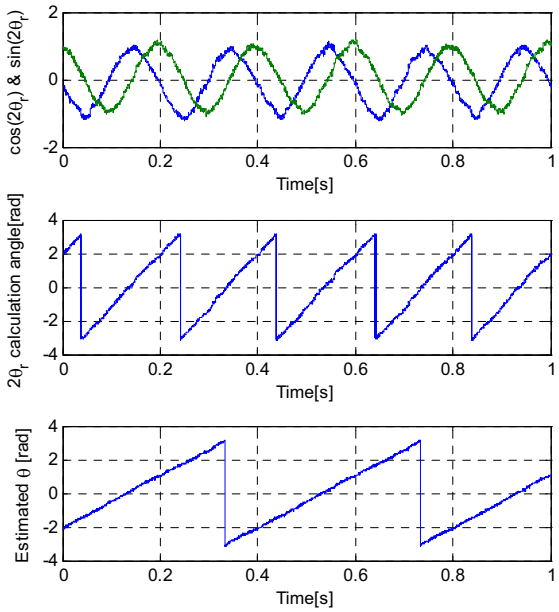

Fig. 6. Rotor position related value from inductance matrix, 2θ calculation result, and estimation angle.

Fig. 6 shows the inductance matrix values, rotor position calculation angle and rotor position estimation result. The first figure in Fig. 5 means the cosine value and the sine value in (17). From these two inductance value, the two times of the rotor position, $2\theta_r$ can be calculated by *atan2* function. From the calculation results, the rotor position can be estimated by a Luenberger speed observer or by a simple state filter

IV. Experimental Results

To verify the performance of the proposed method, an 11kW IPMSM drive system coupled to a load machine was used. Parameters of the IPMSM are listed in Table. I. Three phase PWM inverter whose DC link voltage is 300V DC-link was used to drive the IPMSM. PWM switching frequency is 10kHz and current sampling frequency is 20kHz. The high frequency voltage signal shown in Fig. 3 is injected. And, the frequency of the injected signal is 6.67kHz and its magnitude is 40V. The

rotor position information was calculated with only three sampling currents and voltages as (16) and (18).

Fig. 7(a) shows the FFT results of phase current. Before voltage signal injection, there are only PWM switching frequency component, about 200mA. With the injection of the signal, the 400mA, 6.67kHz component appears in the spectrum of the phase current. Using this current component, the rotor position can be calculated. As shown in Fig. 7(b), under the step change of q-axis current reference in the rotor reference frame, the error between calculated position and real position kept within +/-0.2radian after transient. From Fig. 7(c), it can be seen that the current regulation bandwidth with the proposed sensorless control is around 300Hz.

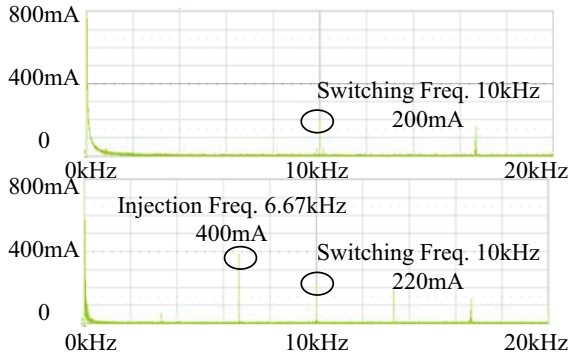

(a)

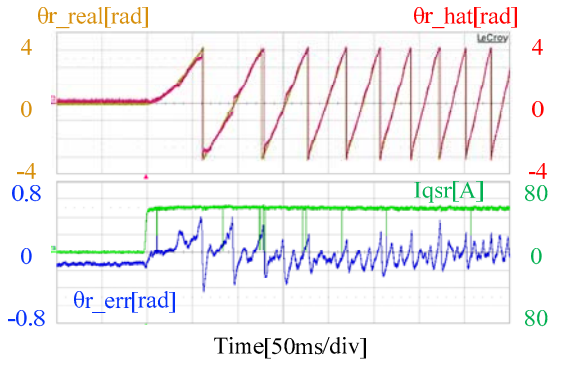

(b)

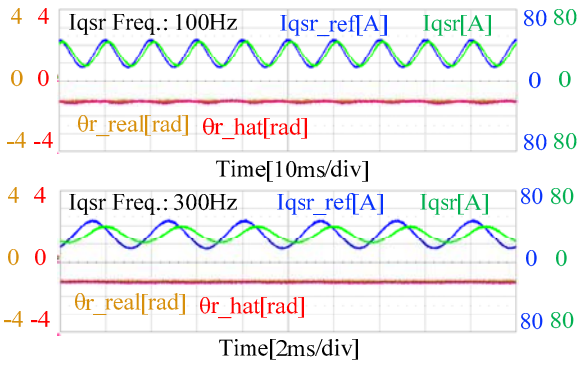

(c)

Fig. 7. Experimental results in the proposed sensorless method. (a) Phase current FFT results. Upper shows the FFT without signal injection. Only PWM ripple currents exist. Bottom shows the FFT with signal injection. At 6.67kHz, 400mA component exists. (b) Step change of reference of q-axis current by rated value. (c) Sinusoidal reference. Upper figure: 100Hz sinusoidal current reference. Offset current is 30A, Magnitude of sinusoidal wave is 15A. Bottom figure: 15A 300Hz sinusoidal and 30A offset current reference.

The speed control performance is shown in Fig 8. Speed control bandwidth is 25Hz and the bandwidth of the speed observer is 25Hz. To verify the speed estimation performance, the real rotating speed was measured by encoder signal. The Under the step change of the speed reference, and the sinusoidal speed reference whose frequency is 5Hz and 15Hz, the actual speed tracks well its reference.

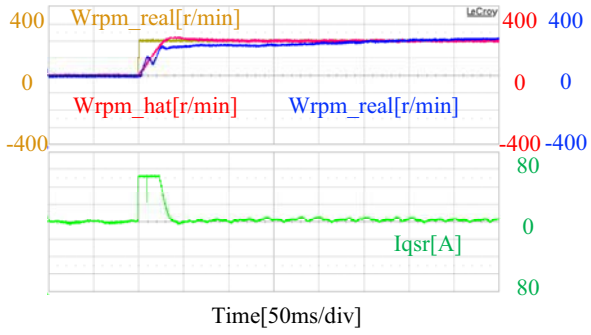

(a)

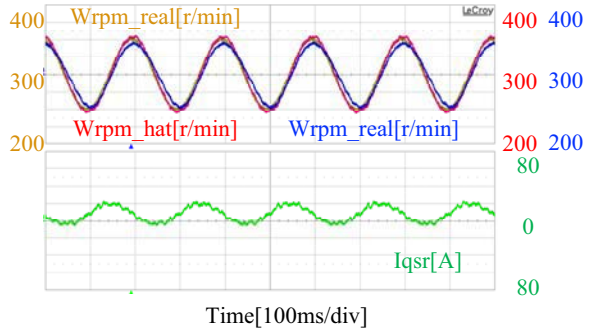

(b)

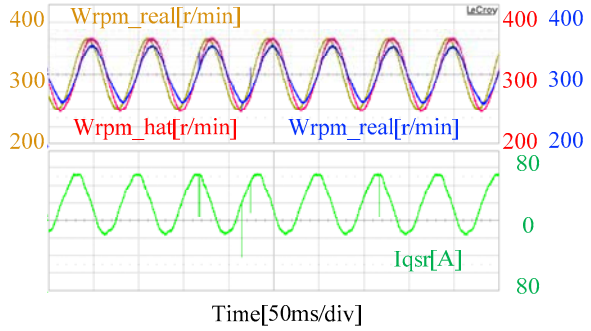

(c)

Fig. 8 Experimental results with the proposed sensorless method. Speed control bandwidth is set as 25Hz. (a) Speed control performance: from standstill to 200r/min step response. At beginning, the current reference was saturated. (b) Speed control with 5Hz sinusoidal speed reference. (c) Speed control with 15Hz sinusoidal speed reference.

TABLE I
IPMSM AND SYSTEM PARAMETERS FOR EXPERIMENTAL TEST

Quantity	Value [Unit]
Rated Power	11 [kW]
Rated Rotating Speed	1750 [r/min]
Rated Phase Current	39.5 [Arms]
Stator Resistance, R_S	0.15 [Ω]
Flux linkage of Permanent Magnet	0.249 [V·s]
Inductance, (L_d, L_q)	3.4 / 4.6 [mH]
Sampling Frequency	20 [kHz]
PWM Switching Frequency	10 [kHz]
Injection Signal Frequency	6.67 [kHz]
Injection Voltage Signal Magnitude	40 [V]
DC-link Voltage	300 [V]

V. CONCLUSIONS

This paper has proposed a new position sensorless method based on the high frequency signal injection and the frequency of the injected signal is increased up to two third of PWM switching frequency. Because of this high injection frequency, the dynamics of the sensorless control can be improved. Furthermore, the audible noise is reduced conspicuously. This method does not need any high frequency filter and use only three successively sampled currents and voltages with three voltage vectors in a period of the injected signal. The voltage vectors are rotating at the stationary reference frame. The rotor position is directly calculated by the sampled currents and voltages in a period of injected signal. The 15Hz speed control bandwidth and 300Hz current regulation bandwidth has been demonstrated with the experimental set-up based on M-G set.

REFERENCES

[1] P. L. Jansen, and R. D. Lorenz, "Transducerless position and velocity estimation in induction and salient AC machines," *IEEE Trans. Ind. Appl.*, vol. 31, no. 2, pp. 240-247, Mar./Apr. 1995.

[2] N. Matsui, "Sensorless operation of brushless DC motor drives," in *Proc. IEEE IECON'93*, 1993, pp. 739-744.

[3] S. Morimoto, K. Kawamoto, M. Sanada, and Y. Takeda, "Sensorless control strategy for salient-pole PMSM based on extended EMF in rotating reference frame," *IEEE Trans. Ind. Appl.*, vol. 38, no. 4, pp. 1054-1061, Jul./Aug. 2002.

[4] B.-H. Bae, S.-K. Sul, J.-H. Kwon, and J.-S. Byeon, "Implementation of sensorless vector control for super-high-speed PMSM of turbo-compressor," *IEEE Trans. Ind. Appl.*, vol. 39, no. 3, pp. 811-818, May/Jun. 2003.

[5] M. J. Corley, and R. D. Lorenz, "Rotor position and velocity estimation for a salient-pole permanent magnet synchronous machine at standstill and high speeds," *IEEE Trans. Ind. Appl.*, vol. 34, no. 4, pp. 784-789, Jul./Aug. 1998.

[6] J.-I. Ha, and S.-K. Sul, "Sensorless field-orientation control of an induction machine by high-frequency signal injection," *IEEE Trans. Ind. Appl.*, vol. 35, no. 1, pp. 45-51, Jan./Feb. 1999.

[7] M. Schroedl, "Sensorless control of AC machine at low speed and standstill based on the 'INFORM' method," in *Conf. Rec. IEEE-IAS Annu. Meeting*, 1996, pp. 270-277.

[8] M. Mamo, K. Ide, M. Sawamura, and J. Oyama, "Novel rotor position extraction based on carrier frequency component method (CFCM) using two reference frames for IPM drives," *IEEE Trans. Ind. Electron.*, vol. 52, no. 5, pp. 508-514, Apr. 2005.

[9] R. Leidhold, and P. Mutschler, "Improved method for higher dynamics in sensorless position detection," in *Proc. IEEE IECON2008*, 2008, pp. 1240-1245.

[10] Y.-D. Yoon, S.-K. Sul, S. Morimoto, and K. Ide, "High bandwidth sensorless algorithm for AC machines based on square-wave type voltage injection," in *Proc. IEEE ECCE2009*, 2009, pp. 2123-2130.

[11] F. Briz, M. W. Degner, P. Garcia, and R. D. Lorenz, "Comparison of saliency-based sensorless control techniques for AC machines," *IEEE Trans. Ind. Appl.*, vol. 40, no. 4, pp. 1107-1115, Jul./Aug. 2004.

[12] C. Caruana, G. M. Asher, and M. Sumner, "Performance of HF signal injection techniques for zero-low-frequency vector control of induction machines under sensorless condition," *IEEE Trans. Ind. Electron.*, vol. 53, no. 1, pp. 225-238, Feb. 2006.

[13] D. Raca, P. Garcia, D. D. Reigosa, F. Briz, and D. L. Lorenz, "Carrier-signal selection for sensorless control of PM synchronous machines at zero and very low speed," *IEEE Trans. Ind. Appl.*, vol. 46, no. 1, pp. 167-178, Jan./Feb. 2010.

[14] F. Briz, M. W. Degner, A. Diez, and R. D. Lorenz, "Measuring, modeling, and decoupling of saturation-induced saliencies in carrier-signal injection-based sensorless AC drives," *IEEE Trans. Ind. Appl.*, vol. 37, no. 5, pp. 1356-1364, Sep./Oct. 2001.

[15] F. Briz, M. W. Degner, A. Diez, and R. D. Lorenz, "Static and dynamic behavior of saturation-induced saliencies and their effect on carrier-signal-based sensorless AC drives," *IEEE Trans. Ind. Appl.*, vol. 38, no. 3, pp. 670-678, May/Jun. 2002.

[16] J.-I. Ha, K. Ide, T. Sawa, and S.-K. Sul, "Sensorless rotor position estimation of an interior permanent-magnet motor from initial states," *IEEE Trans. Ind. Appl.*, vol. 39, no. 3, pp. 761-767, May/Jun. 2003.

[17] P. Garcia, F. Briz, M. W. Degner, and D. D.-Reigosa, "Accuracy, bandwidth, and stability limits of carrier-signal-injection-based sensorless control methods," *IEEE Trans. Ind. Appl.*, vol. 43, no. 4, pp. 990-1000, Jul./Aug. 2007.

[18] J.-K. Ha, "Analysis of inherent magnet position sensors in symmetric AC machines for zero or low speed sensorless drives," *IEEE Trans. Ind. Magn.*, vol. 44, no. 12, pp. 4689-4696, Dec. 2008.